

Three-dimensional modelling of water flow due to leakage from pressurized buried pipe

Hong Zhu^{1a}, Limin Zhang^{*1}, Chen Chen^{1,2,3a} and Kit Chan^{1b}

¹Department of Civil and Environmental Engineering, The Hong Kong University of Science and Technology, Clear Water Bay, Kowloon, Hong Kong

²State Key Laboratory of Hydraulics and Mountain River Engineering, Sichuan University, Chengdu, China

³College of Hydraulic and Hydroelectric Engineering, Sichuan University, China

(Received January 13, 2018, Revised July 17, 2018, Accepted July 31, 2018)

Abstract. A three-dimensional model is constructed to simulate water infiltration in an unsaturated slope from a leaking pipe. Adaptive mesh refinement and time stepping are used, assisted by an automatic procedure for progressive steepening of the hydraulic property function for better convergence. The model is justified by comparing the simulated results with experimental data. Steady-state flow is investigated considering various pipe water pressures, locations and sizes of the opening, and soil layering. The opening size significantly affects the soaked zone around the pipe. Preferential flow dominates along the pipe longitudinal direction in the presence of a loose backfill around the pipe.

Keywords: seepage; buried pipes; water infiltration; unsaturated soil; preferential flow; centrifuge test

1. Introduction

Buried water mains, sewers and storm water pipes are critical underground infrastructures in urban areas. During their service, the pipe may become defective due to a missing piece of the pipe wall, connection defects, or other causes (ETWB 2006). Consequently, water leaks from the pipes at a certain leakage pressure, quickly infiltrating into the soil around the pipe. Water infiltration will cause substantial loss of soil suction, which may destabilize the infrastructure involving the pipe. Due to the importance of maintaining the infrastructure at a good condition and associated safety issues, there is an increasing demand to answer some essential questions: how does the leaked water migrate near the opening and how does the saturation zone expand as the leakage water pressure at the opening increases?

Considerable efforts have been made to model behaviour of either soil particles or fluid associated with pipe leakage. Most recently, Cui *et al.* (2011 and 2014) studied fluidization of cohesive soil induced by pipe leakage using a coupled discrete element method and the lattice Boltzmann approach. They revealed that a cavity in the soil near the pipe opening is initially formed by jet flow and develops continuously until the occurrence of rupture on the top of the stacked particles. Cassa and Van Zyl (2013) proposed a mathematical equation to explain the relation between pressure head and leakage area in pipes.

Guo *et al.* (2013) proposed an approximate solution based on the well-known orifice equation for computing the steady-state leakage rate along a line crack. The focus of these prior studies was on two-dimensional problems which in fact implicitly assumed a channel opening (e.g., Zhu *et al.* 2018). In practice, water often leaks from a small-sized hole, which calls for a three-dimensional analysis algorithm for seepage through unsaturated porous media. Key factors such as pipe water pressure and location and size of opening should also be studied.

The typical geological profile of Hong Kong wholly or partly comprises fill, marine deposit, alluvium, completely/moderately decomposed granite and grade III or better rock in a top-down sequence. The depth of each layer varies by sites, depending on the formation history. Fig. 1(a) shows a standard practice of pipe laying in Hong Kong. A trench is excavated to facilitate pipe laying. After the pipe has been installed, the trench should be backfilled. The backfill material around the pipe should be compacted to a relative compaction (RC) of at least 85% within 300 mm above the crown of the pipe. The material above the 300 mm level should be compacted to a RC of at least 95%. Fig. 1(b) shows a simplification of the standard practice in which the backfill soil is assumed to be compacted to RC=85%. A practical alternative as shown in Fig. 1(c) can be adopted for routing and draining leaked water by constructing an erosion-resistant coarse sandy gravel drain surrounding the pipe. The coarse sandy gravel drain has a coefficient of saturated permeability several orders of magnitude larger than the rest soil. The pipe leakage problem therefore involves a soil profile including two adjacent soil types (i.e., silty sand and gravel) with substantial differences in soil-water characteristics and saturated permeability. As the gravel has a really large saturated permeability, once leakage occurs, the gravel will

*Corresponding author, Professor

E-mail: cezhangl@ust.hk

^aPh.D.

^bPh.D. Student

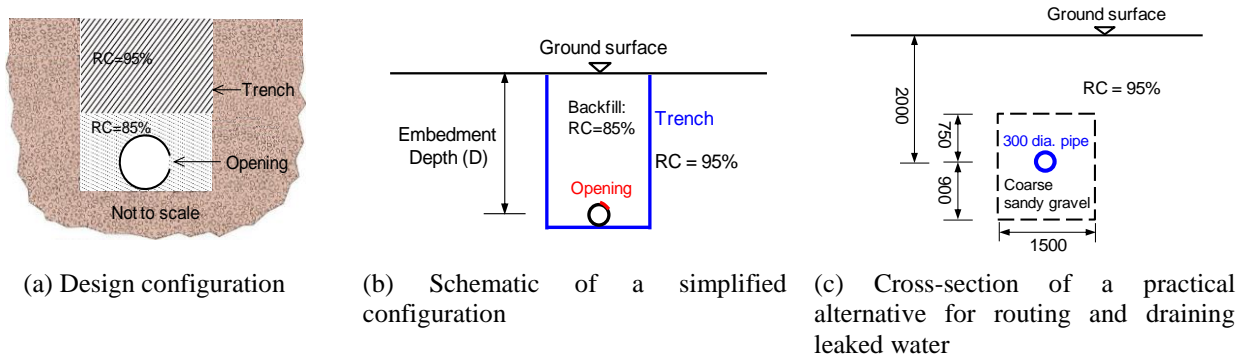


Fig. 1 Standard practice for pipe-laying scheme adopted in Hong Kong

be quickly saturated and the rest silty sand will be gradually saturated, leading to a sharp contrast of the permeability. In dealing with this problem, a computational challenge arises with respect to the treatment of sudden drops in soil permeability at the interface, which may cause the numerical solution to diverge. Although various numerical methods have been applied to model seepage through unsaturated soil (e.g., Bathe and Khoshgoftaar 1979, Lacy and Prevost 1987, Shen and Xu 2011, Zhu *et al.* 2013, Ali *et al.* 2014, Zhu and Zhang 2015, Wu *et al.* 2015, Cui *et al.* 2016, Li *et al.* 2016, Shen *et al.* 2017), it has been widely recognized that numerical solutions to unsaturated flow problems with highly non-linear and steep hydraulic property functions are plagued with convergence difficulties, particularly at the interface of soils with a sharp contrast of permeability (Lam *et al.* 1987, Paniconi and Putti 1994, Baker 2006, Phoon *et al.* 2007, Cheng *et al.* 2008, Szymkiewicz 2012). When pertaining to the problem of pipe leakage in three dimensions, the convergence problem might be severer due to the imposed rapid changes in hydraulic properties in all directions by leakage. In light of such complex problems, adaptive refinement of time-step and element size are both demanded to efficiently solve the leakage problem.

The objectives of this paper are to build a three-dimensional model to simulate water flow induced by leakage of pipes embedded in unsaturated soil through a scheme of adaptive refinement of element size and time-step, assisted by an automatic procedure for progressive steepening of the hydraulic property function; to verify the proposed numerical model using data from a centrifuge model test; and to investigate the steady-state flow regime under the influences of various pipe water pressures, locations and lengths of pipe opening, and the difference of the density of the soils inside and outside the trench.

2. Theory of unsaturated-saturated water flow

2.1 Water flow through unsaturated soil

Taking account of continuity and Darcy's law conjunctively leads to the partial differential equation that governs the water flow in three-dimensional unsaturated soil (Richards 1931)

$$\frac{\partial}{\partial x} \left(k_x \frac{\partial h}{\partial x} \right) + \frac{\partial}{\partial y} \left(k_y \frac{\partial h}{\partial y} \right) + \frac{\partial}{\partial z} \left(k_z \frac{\partial h}{\partial z} \right) = - \frac{\partial \theta}{\partial t} \quad (1)$$

where k_x , k_y and k_z are the coefficients of permeability in the x -, y - and z - direction, respectively; h is the hydraulic head; θ is the volumetric water content; and t is the elapsed time. The coefficient of permeability can be assumed to be constant for saturated soil, but is a function of soil suction (i.e., negative pore-water pressure) for unsaturated soil and decreases with an increase in soil suction. The relationship between the coefficient of permeability of unsaturated soil and soil suction is referred to as a permeability function. Under a steady state, the time-dependency of hydraulic head profile is eliminated by removing the term on the right-hand side of Eq. (1). Obtaining pore-water pressure profile in three dimensions involves solving the partial differential equation, which requires both an unsaturated permeability function and a soil-water characteristic curve (SWCC) for the unsaturated soil.

2.2 Soil hydraulic property function

The soil-water characteristic curve (SWCC) developed by Fredlund and Xing (1994) is used,

$$\theta = C(\psi) \frac{\theta_s}{\left\{ \ln \left[e + (\psi/a)^n \right] \right\}^m} \quad (2)$$

where θ_s is the saturated volumetric water content; e is the natural base of logarithm; a is the matrix suction at the inflection point of the curve which is closely related to the air-entry value (i.e. the suction beyond which the soil starts to desaturate); n is a parameter that controls the slope at the inflection point of the soil-water characteristic curve; m is a parameter related to the soil residual water content; ψ is the soil matric suction; $C(\psi)$ is a correction function which is often taken as one.

An exponential equation describing the coefficient of permeability as a function of soil matric suction, developed by Leong and Rahardjo (1997), is employed

$$k = k_s \left(\frac{\theta - \theta_r}{\theta_s - \theta_r} \right)^q \quad (3)$$

where k_s is the coefficient of saturated permeability; θ is the volumetric water content; θ_r is the residual volumetric water content at which a large suction is required to remove additional water from the soil; $(\theta - \theta_r) / (\theta_s - \theta_r)$ is the normalized water content; q is a coefficient depending on the soil type.

3. Three-dimensional model for a slope involving a leaking pipe

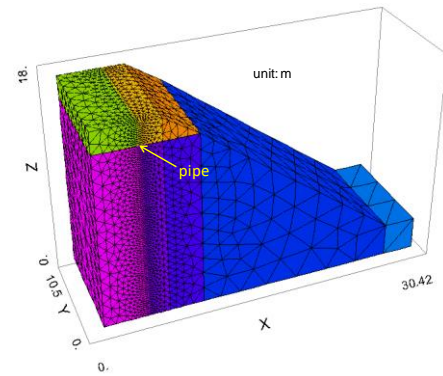
3.1 Model creation and adaptive mesh generation

This study makes use of FlexPDE (PDE Solutions Inc. 2005) a scripted tool for establishing finite element model, to efficiently solve the partial differential governing equation and then to obtain the hydrological response to pipe leakage within the slope. Fig. 2(a) shows the finite element mesh created for the proposed infiltration analysis. Fig. 2(b) shows an arbitrary cross-sectional view of the model to facilitate the illustration of the model creation. The model is composed of four surfaces from the bottom to the top with each two consecutive surfaces forming a layer, numbered sequentially. For example, layer 1 comprises surface 1 at the bottom and surface 2 at the top; layer 3 is formed by setting surface 3 at the bottom and surface 4 at the top. As such, the buried pipe layer is modelled at layer 2 with both of the two surfaces connecting to the slope boundaries. The cylindrical pipe region is assigned as a void equivalent to the air so that no flow is allowed to enter/exit the pipe surface. Regions other than the pipe are all specified with the soil material.

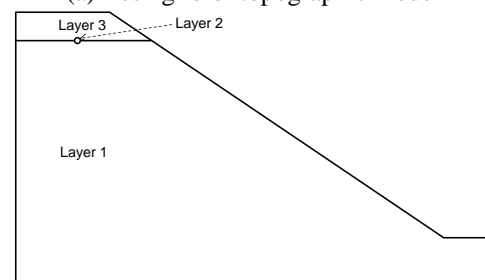
The region of the pipe is only 300 mm in diameter, which is very small compared to the whole analysis domain. Non-uniform cell spacing must be applied to different regions, with smaller spacings for the pipe and larger spacings for the rest region. Adaptive mesh auto-generation is allowed in such a way that the pipe of an extremely small volume compared to the whole model is re-gridded at much smaller mesh spacings than the region outside the pipe. FlexPDE is able to identify the critical zone and automatically refine the mesh in the critical zone with an objective of attaining good convergence. An example would be when boundary surfaces for different zones intersect, forming irregular and sharp elements. Featured polygons specifically designed to smoothen the irregular elements are added correspondingly, which enables the mesh to be re-gridded to ensure acceptable accuracy.

3.2 Staged analysis approach for steady-state problems and adaptive mesh and time-step refinement for transient-state problems

A highly nonlinear and steep permeability function is commonly encountered for sandy or gravelly soils. High nonlinearity means that the function associated with a problem includes a term with power of three or above with respect to the variable, or that the change of the slope of the curve expressing the function exhibits no significant regularity. The solution to the problem is hard to be expressed in an explicit way. As pointed out by Lam *et al.*

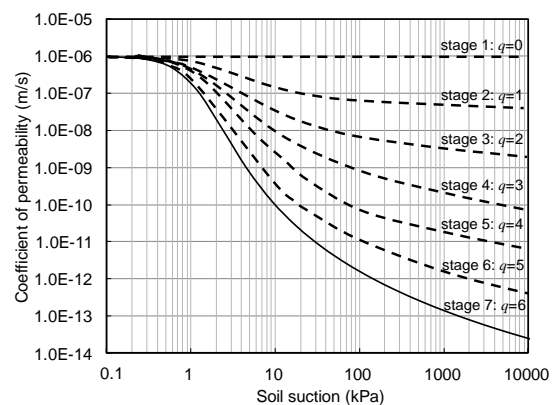


(a) Mesh grid of topographic model

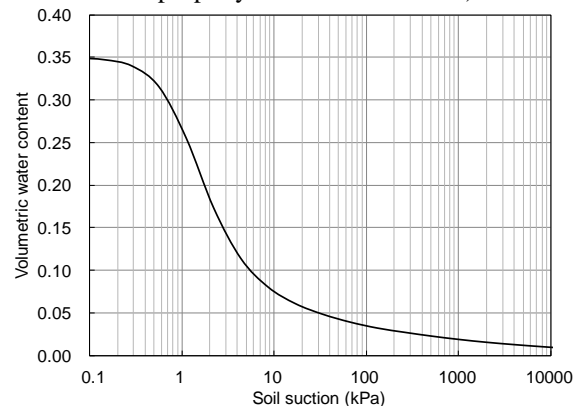


(b) An arbitrary cross-sectional view of the model

Fig. 2 Creation of the three-dimensional slope with a buried pipe



(a) Permeability function steepened following stage 1 to stage 7 for addressing numerical instability (solid line denotes the true property function for the soil)



(b) Soil-water characteristic curve

Fig. 3 Hydraulic property functions for the silty sand compacted at 95% degree of compaction referring to Yin (2009)

(1987), a permeability function is regarded as moderately steep when an increase of every 50 kPa of soil suction corresponds to a decrease of at least one order of magnitude in the coefficient of permeability. Fig. 3 shows the permeability function and SWCC for the silty sand according to Yin (2009). The solid line in Fig. 3(a) shows a permeability function for a sandy soil, which is represented by Eq. (3) with q equal to 6. According to the definition given by Lam *et al.* (1987), the permeability function is steep, which could easily lead to divergence of the steady-state solution for three-dimensional seepage problems.

An approach for staged analysis is therefore proposed. In each new stage, the result of the previous stage is used as its initial condition. This is technically termed “preconditioning of convergence” (Wood 1993) useful for solving highly non-linear problems. The solution of the steady-state problem that satisfies a convergence criterion can be obtained by using staged permeability functions. Fig. 3(a) shows the staging of permeability function. At the initial stage, a flat curve corresponding to a constant saturated permeability is used. It is further steepened at subsequent stages until at the final stage the actual steep permeability function is approached. The more stages that are involved in the staging of the permeability function, the more accurate the solution will be. Jointly considering the time cost and computation effort leads to an optimal number of stages to be used. The staged permeability functions are represented by staged values of the exponent (i.e., q) in the permeability function in Eq. (3). The corresponding analyses are run in multiple successive sessions. Fig. 3(b) shows the corresponding SWCC for the same type of soil which is not staged in the analysis.

The algorithm written and performed in FlexPDE is capable of integrating adaptive time-step size and mesh refinement for solving transient problems and thus provides added degrees of convergence stability for the solution. The time-step size is initially very small and increases gradually at a varied rate depending on the magnitude of produced time error relative to the default maximum allowable error. For instance, if the produced error is relatively small, the time-step size will be enlarged automatically to cater for the desired calculation efficiency; when the allowable error is approached, the time-step size is automatically reduced to refine the model to obtain an acceptable error below the limit.

4. Verification of the numerical approach with centrifuge test

4.1 Geometry of the slope and pipe

To gain a physical insight of the effect of pipe bursting on the water movement in a slope, a centrifuge test has been conducted in the Hong Kong University of Science and Technology to reproduce the prototype stress conditions and model the pipe bursting as well as the associated groundwater conditions under the influence of pipe leakage at various time steps.

As an integral part of our project, the numerical scheme is developed in conjunction with a centrifuge model test

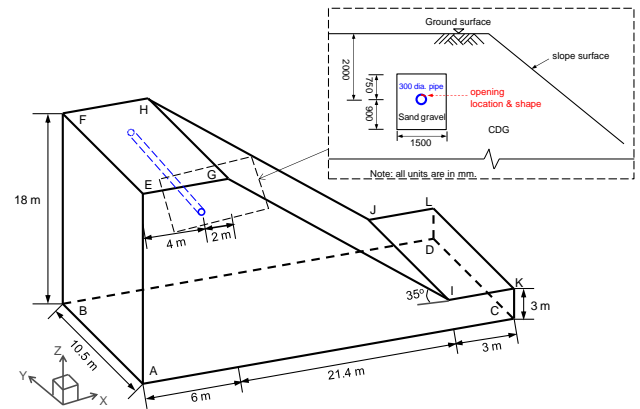


Fig. 4 Geometry of the slope and the close-up view of the region surrounding the pipe

Table 1 Soil parameters adopted in the numerical analysis

Parameter	Definition	Value
k_{s1} (m/s)	Saturated permeability for CDG at RC=95%	1.0×10^{-6}
k_{s2} (m/s)	Saturated permeability for CDG at RC=85%	5.0×10^{-5}
q	The exponent of Leong and Rahardjo (1994) permeability function	6
θ_{s1}	Saturated volumetric water content for the CDG at RC=95%	0.35
θ_{s2}	Saturated volumetric water content for the CDG at RC=85%	0.45
θ_{ss}	Saturated volumetric water content for the sand gravel surrounding the pipe corresponding to the test condition.	0.38
a (kPa $^{-1}$)		1
n	Fitting parameters for the Fredlund and Xing (1994) model	2
m		1

Note: The saturated permeability and the saturated volumetric water content for the CDG soils at RC=85% and RC=95% are referenced to GEO report (1977), Yin *et al.* (2009) and Yoon *et al.* (2016) conjunctively.

designed and performed by a co-author of this paper. The fluid used in the centrifuge test was tap water, which is the same as the fluid in the water supply pipes. The physical phenomenon concerned is water infiltration, which is governed by Darcy's law and mass conservation. Therefore, the scaling of the fluid flow should be in compliance with diffusion/consolidation, and the natural water should be used as the modeling fluid. In the centrifuge experiment, Darcy's flow is valid as turbulent flow is unlikely to occur due to slow flow velocity and small particle size, which ensure small Reynold's number. Given the validity of the scaling laws, the centrifuge model is meaningful and can represent the prototype slope. Note that an artificial fluid with increased viscosity should be used for modeling dynamic problems on centrifuges.

In the centrifuge experiment, several schemes of protection measures for the pipe are explored to minimize possible jet erosion and prevent damage to the pipe. One of the schemes suggested the provision of a coarse sandy gravel layer around the pipe. The pore-water pressure responses were continuously monitored during the test

period. To be in line with the centrifuge model test, the model geometry in the numerical analysis is specified to be identical to the geometry of the centrifuge model. Given that the test result is well monitored over time and the properties of the test soil are available for the numerical simulation, the authors choose to validate the numerical approach using the existing centrifuge model test. This section first presents an analysis case utilizing the presented numerical approach. The numerical results in terms of the pore-water pressure distribution at a specific elapsed time are extracted from the transient process and overlaid with the observations captured from the centrifuge test using a coarse sandy gravel layer as a protection measure.

The geometry of the slope and pipe is set to represent a practical case. As shown in Fig. 4, we consider a 15 m high slope inclined at 35 degrees. The slope consists of completely decomposed granite (CDG), which is classified as silty sand. The compacted soil may be anisotropic and exhibit a certain degree of heterogeneity due to soil inherent variability (e.g., Xiao *et al.* 2017, Phoon 2017). Since the degree of anisotropy is not measured in this study and the focus is to investigate the influence of details about the pipe leakage on the pore-water pressure distributions over the whole slope region, the soil is assumed to be isotropic with the same saturated permeability value for the same degree of compaction. A pipe 300 mm in diameter (a typical size of water supply pipe used in practice) is embedded at a depth of 2 m that represents the common pipe-laying practice in Hong Kong. The out of plane length of the pipe is assumed to be 10.5 m. The type of soil in the region surrounding the pipe is made of coarse sandy gravel with saturated permeability coefficient several orders of magnitude larger than the soil compacted in the rest of regions. To reflect the coarse sandy gravel zone, a close-up view including the cross-section of the pipe, the coarse sandy gravel and the portion that covers this highly permeable layer is also provided in Fig. 4. This coarse sandy gravel zone encompasses a cross-sectional area of 1.5 m × 1.65 m, extending all through the out-of-plane direction (i.e., pipe longitudinal direction). The location of the leakage opening is shown in Fig. 4, the arc length of opening accounting for 12.5% of the pipe perimeter at the cross-section.

In line with the centrifuge model, all the boundaries in the numerical model are impermeable except for the surface which is a free-exit boundary; any positive pore-water pressure developed at the ground surface is taken as zero. Leakage from the pipe is simulated by applying a constant hydraulic pressure, the magnitude of which is equal to the operating pressure inside the pipe. A constant water pressure of 35 kPa is applied to the opening, the same as the applied value in the centrifuge model. The transient infiltration process lasts for a period of 37 days, corresponding to the realistic duration that the centrifuge test reflects in prototype. The duration of 37 days is selected because the leakage pressure was held constant within this period in the centrifuge test. The pore-water pressure readings in the centrifuge test were taken from six pore-water pressure transducers (PPT) that were properly aligned within the slope in the vicinity of the middle slope section. As the coarse sand gravel has a large permeability (i.e., at the order of 10^{-3} m/s reported by Revil and Cathles (1999) and Zhang *et al.* (2016)), upon leakage the gravel will be

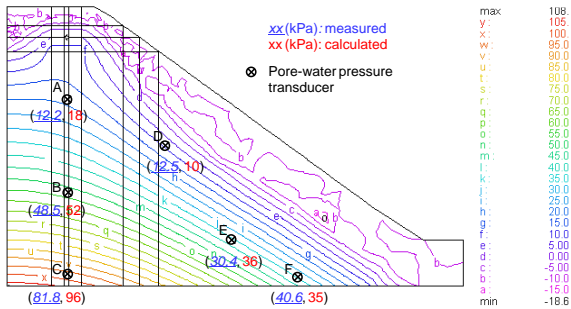
quickly saturated, and the rest silty sand will be saturated gradually later. This consideration leads to the treatment of the gravel layer as a saturated material and a new drainage boundary at the gravel-CDG interface. The hydraulic properties of the compacted CDG at 95% degree of compaction are indicated by the solid lines in Fig. 3. The coefficient of saturated permeability and the fitting parameters for the permeability function and SWCC are summarized in Table 1, with reference to published values by Geotechnical Engineering Office (1997), Yin (2009) and Yoon *et al.* (2015). The transient problem is governed by the partial differential equation described in Eq. (1). Solving the time-dependent equation requires the input of initial conditions for the problem. According to the measurement of the initial suction within the slope prior to the onset of leakage, a suction value of 10 kPa was recorded over the entire slope.

4.2 Convergence problem with conventional analysis

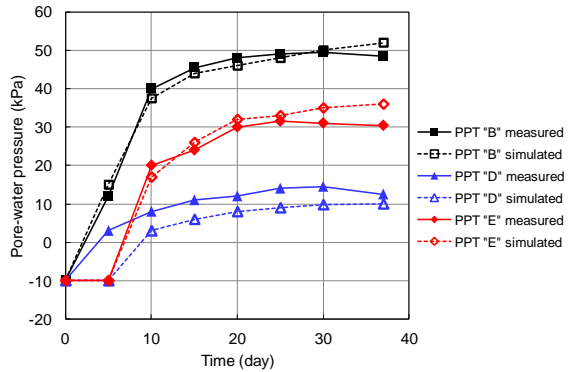
To demonstrate the need for staged analysis to handle the steep hydraulic function in the three-dimensional leakage problem, an analysis case for the problem described in section 4.1 is conducted which adopts a non-staged option straightforwardly using the actual steep unsaturated hydraulic function. The coarse sandy gravel has very large saturated permeability (i.e., 10^{-3} m/s), which is in sharp contrast with the unsaturated silty sand with an initial permeability on the order of 10^{-10} m/s according to the measured initial suction at 10 kPa and the permeability curve in Fig. 3(a). It turns out that the process is unable to proceed, showing a significant degree of divergence. The estimated relative error exceeds the limit (i.e., 0.01), a common value of the limit suggested for the three-dimensional case to control the convergence of the solution. The non-staged skill is not able to make the analysis error below the required limit and some excursions occur. Therefore, the internally embedded function of staging in FlexPDE is utilized. It has the benefit of allowing users to use the staging capability to gradually activate the nonlinear item. The analysis starts with a linear system, finds a solution that is consistent with the boundary condition, and then uses this solution as a starting point for a more strongly nonlinear problem. As such, pre-conditioning in the form of staged hydraulic function offered by FlexPDE is performed.

4.3 Verifying the numerical approach with the centrifuge test

After specifying all the conditions of the slope following those designed in the centrifuge test, the transient analysis has been conducted for a period of 37 days. The calculated pore-water pressure contours at the middle slope section are extracted at time intervals of 5 days or shorter. The contours at the end of the 37-day duration are presented in Fig. 5(a). The simulated values of the pore-water pressures at the locations of the PPTs are compared with the test readings. Both the locations of the PPTs and the readings are shown on the contours to help understand how the comparison is conducted. Taking the results at the end of duration as an example, the experimental values and the simulation values



(a) Pore-water pressure contour at the end of 37 days



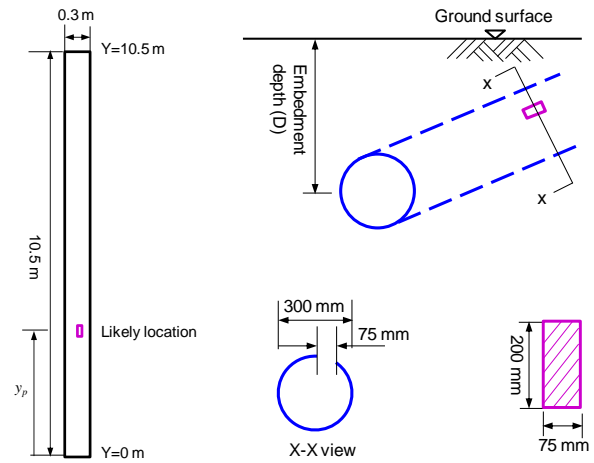
(b) Variation of pore-water pressure values along 37 days of test duration since the onset of leakage

Fig. 5 Comparison of the computed and measured results

are presented in pair in the bracket. The calculated values agree well with the observed values at the moderate height (PPTs “B” and “D”), with deviations of 7% and 20%, respectively. The maximum difference is observed at the top PPT (location “A”), which may be attributed to the close proximity of this PPT to the bursting point, leading to unstable readings to some extent. The numerical responses at the bottom three PPTs (locations “C”, “E”, and “F”) only deviate 17%, 18% and 14%, respectively, from the actual readings. Fig. 5(b) compares the results over the entire test duration. For enhanced clarity, the PPT readings and the simulated results are shown for the three PPTs at the medium height only. The simulated and experimental trends of variation against time for PPTs “B” and “E” are quite consistent. For PPT “D”, within the initial five days, the measured value increases but the simulated one remains at -10 kPa. It is speculated that lateral preferential flow occurs during the test at the height of PPT “D”, likely due to the non-uniform compaction of the soil sample. As the process proceeds, the trends become similar and the values do not differ obviously. As a whole, the simulated results show reasonable agreement with the observed results in the centrifuge test. The slight discrepancy of the values is due to several causes: preparation of the test sample on a layer by layer basis in which perfect consistency among each layer may not be quarantined; unavoidable errors in reading; and imperfect control of test equipment. Given the good agreement, the numerical approach is hence deemed appropriate for modelling the leakage process. In order to fully investigate how the key factors such as pipe water pressure, leakage location and the standard practice with relatively loose soil encompassing the pipe, the following sections will deal with steady-state flows in the slope.

Table 2 Analysis cases for the proposed study

Case No.	Controlling parameter	Values	Remarks
1	Pipe water pressure (p : kPa)	1, 5, 40	$y_p=0.1$ m and $l_p=0.2$ m
2	The length of opening (l_p : m)	0.2, 1, 5	$p=20$ kPa
3	The location of opening (y_p : m)	0.1, 2.1, 5.1	$p=20$ kPa and $l_p=0.2$ m
4	Relative compaction of the backfill material	95% , 85%	$p=20$ kPa, $y_p=0.1$ m and $l_p=0.2$ m



(a) Plan view of the pipe (b) Cross-sectional view of the pipe and opening

Fig. 6 Details of the pipe alignment and the geometry of the opening

5. Investigating effect of pipe bursting on suction regimes using staged analysis

5.1 Details of pipe dimensions and opening

Fig. 6 shows the details of the pipe alignment and the dimensions and locations of the rectangular-shaped opening. Fig. 6(a) shows a plan view indicating one possible location of the single opening that may occur anywhere along the longitudinal direction. The location is quantified by ‘ y_p ’, denoting the distance between the opening and the pipe end (i.e., the impermeable wall). The arc length of the opening in the cross-section outlined in Fig. 6(b) is equal to 12.5% of the total perimeter length, which is kept constant throughout the entire study. The length of the opening as indicated in Fig. 6(c) is assumed to be 200 mm, with an area of about 235.5 cm². It is worth noting that the opening length that basically determines the amount of water released from the pipe could be a key factor that potentially influences the steady-state pore-water distribution. The effect of various opening lengths is investigated. Note that we focus on storm water pipes and sewage pipes. Such pipes are embedded at a depth of approximately 2 m and the pipe pressures generally do not exceed 40 kPa. As such, the simulated pipe pressure is limited to a maximum of 40 kPa. Various leakage water pressures ranging from 1 kPa to 40 kPa are simulated. Furthermore, the influences of the location of opening are studied as indicated in Fig. 6(a).

Table 2 summarizes four cases that cover the effect of pipe water pressure, the length and location of the opening, as well as the relative degree of compaction of the backfill material on the flow regime. The preferential flow in the loosely compacted soil is given particular attention. Case 1 aims to study the influence of pipe water pressure by simulating three values of pipe water pressures; namely 1 kPa, 5 kPa and 40 kPa. The location of the opening is assumed to be fixed at the middle of the pipe at the crown (i.e., $y_p=0.1$ m in Fig. 6(a)). Case 2 intends to investigate the impact of the length (l_p) of opening which controls the quantity of leaked water. In case 2, the pipe water pressure

is specified at 20 kPa. One end of the opening is set at the pipe end and the length of the opening for each scenario varies (i.e., 0.2 m, 1 m and 5 m). Case 3 is devised to evaluate the effect of the location of the opening expressed in terms of y_p on the flow regime. Since the model is symmetric around the center of the pipe, the value of y_p is extended only to 5.1 m. Unlike cases 1-3 in which the whole soil profile is treated as RC=95% soil, case 4 simulates the backfill CDG soil within the trench (Fig. 1(b)) at RC=85%, forming a heterogeneous soil profile. Particular attention is paid to the preferential flow in the relatively loose soil layer. In this case, the opening is fixed at $y_p=0.1$ m with a pipe water pressure equal to 20 kPa.

The study considers a simplified configuration assuming a uniform relative compaction for all the backfill material consistently over the region as indicated in Fig. 1(b). The different degrees of compaction between the two zones inside and outside the trench lead to a contrast in the soil permeability function and SWCC. In the present study, two cases will be compared: one with a relative compaction of the backfill equal to that of the rest region representing a homogeneous soil profile and the other with a relative compaction of the backfill smaller than that of the rest soil denoting a heterogeneous soil profile.

5.2 Results and discussions

5.2.1 Influence of pipe water pressure

Three-dimensional analyses are conducted to investigate the influence of pipe water pressure from the leakage opening on the pore-water pressure (u_w) distribution in the zone surrounding the pipe. For this purpose, three pressure values (i.e., 1 kPa, 5 kPa and 40 kPa) are simulated at the opening fixed at $y_p=0.1$ m on the crown of the pipe, with reference to Fig. 6 for the exact geometry of the pipe and the details of leakage opening. Fig. 7 shows the u_w contours along the pipe longitudinal direction for the three water pressures simulated. The suction decreases as the leaked water infiltrates into the soil; the magnitude of reduction depends on the pressure applied to the opening. It is evident that the closer to the opening, the higher the hydraulic gradient can be induced as captured by the dense contour lines towards the opening location. For applied water pressures equal to 1 kPa and 5 kPa, the soaked zone is very limited and there is no significant difference in the groundwater elevation. It is attributed to the small difference of the pressures within the same order which is not large enough to alter the groundwater table. As the water pressure increases to 40 kPa, the soaked zone extends downward about 1 m below the pipe. The greater the

leakage pressure is, the more mounded the groundwater table will be.

5.2.2 Influence of opening length

The size of the opening hole is always uncertain owing to the attributes and working conditions of the pipe, which determines the amount of water released from the pipe. To investigate how the size affects the propagation of wetting front, the length of the opening hole is selected as a parameter, which takes the values of 0.2 m (i.e., a small hole), 1 m and 5 m (i.e., a long fracture). The pore-water pressure distributions in the lateral direction subject to the three opening lengths are shown in Fig. 8. For the small fracture, $l_p=0.2$ m, shown in Fig. 8(a), only a very limited region near the opening is fully soaked and the groundwater table only rises to an elevation of 4 m. The limited amount of water released from the small hole moves downwards and joins the groundwater. As the leakage develops from a hole to a long fracture, the soaked zone near the opening becomes larger, laterally equal to the opening length and vertically extending to 2 m below the pipe. The rise of the groundwater table for the long fractured opening length appears to be twice that for the very small opening length as a hole. The reductions of suction are more substantial for larger opening lengths than smaller ones. Figs. 8(a)-8(c) display the same observation that the groundwater condition directly under the pipe is influenced more significantly than away from the pipe. Note that in reality the pipe pressure will decrease substantially when a long fracture develops. The analysis results in Fig. 8 hence overestimate the impact.

5.2.3 Effect of opening location along the longitudinal direction

The location of the opening may not be easily detected using current techniques in practice due to that the embedded pipe is hardly visible. Visual inspection of the wet spotted area on the surface ground has usually been relied on for detecting any suspicious pipe leakage, which however maybe sometimes too late to prevent possible severe consequences. To investigate how changes in the location of opening affect pore-water pressure regime, a series of numerical studies has been conducted considering three locations of opening located at $y_p=0.1$ m, 2.1 m and 5.1 m (i.e., at the middle of pipe) with the length of the opening fixed at 0.2 m. Fig. 9 shows the pore-water pressure contours for the three scenarios at the cross-section along the pipe longitudinal direction. Regardless of the leakage location, the groundwater table is maintained at the same elevation. The maximum suction that is remained at the ground surface under the influence of leakage changes in a descending order when the opening location changes from $y_p=0.1$ m to $y_p=5.1$ m. This observation might be due to that the dissipation of suctions is greatly affected by the boundary extent given the non-permeable boundary condition at the pipe ends. It is inferred from the density of the contours that the area closer to the leakage opening experiences a more rapid reduction of suction than that situated far away, which indicates a critical zone around the pipe opening that may trigger soil mass instability.

5.2.4 Impact of backfill material density zoning in the trench

The previous sections present and compare possible

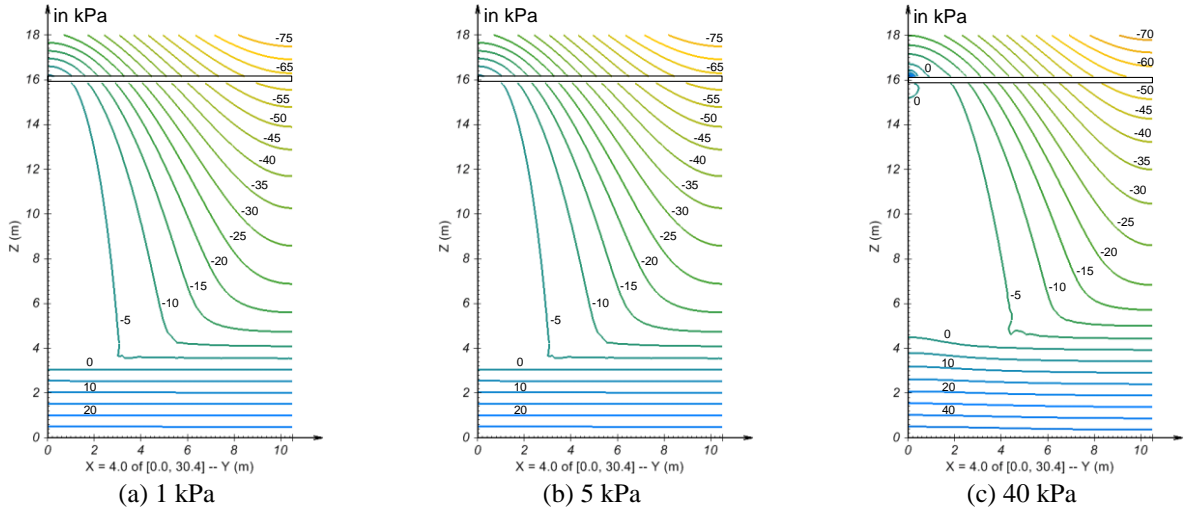


Fig. 7 Comparison of steady-state pore-water pressure contours in uniform soil at 95% relative compaction along the pipe direction subject to various pipe water pressures for the opening fixed at the pipe end

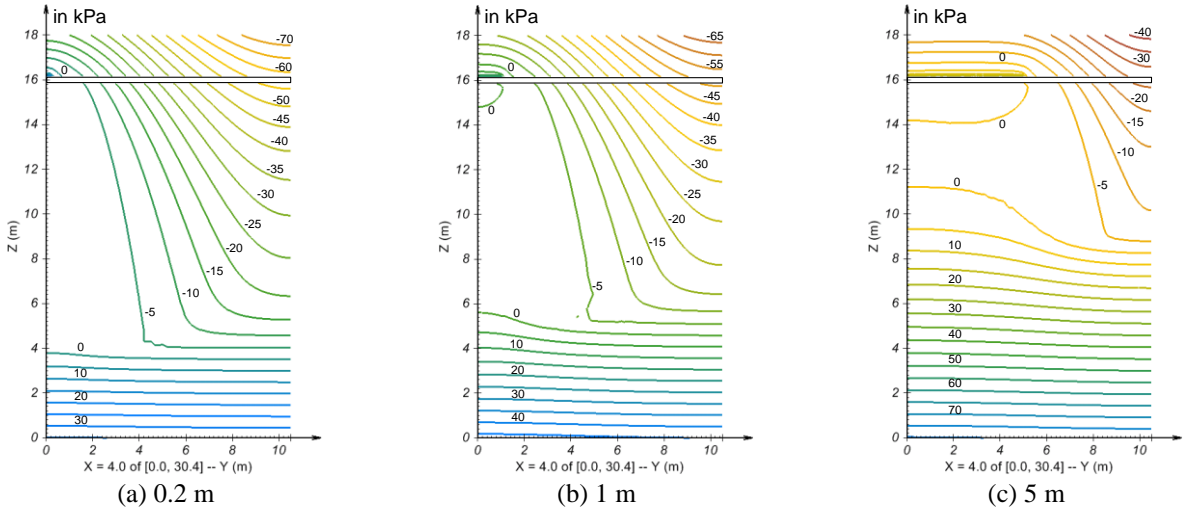


Fig. 8 Comparison of steady-state pore-water pressure contours in uniform soil at 95% relative compaction along the longitudinal direction for $p=20$ kPa with different fracture lengths

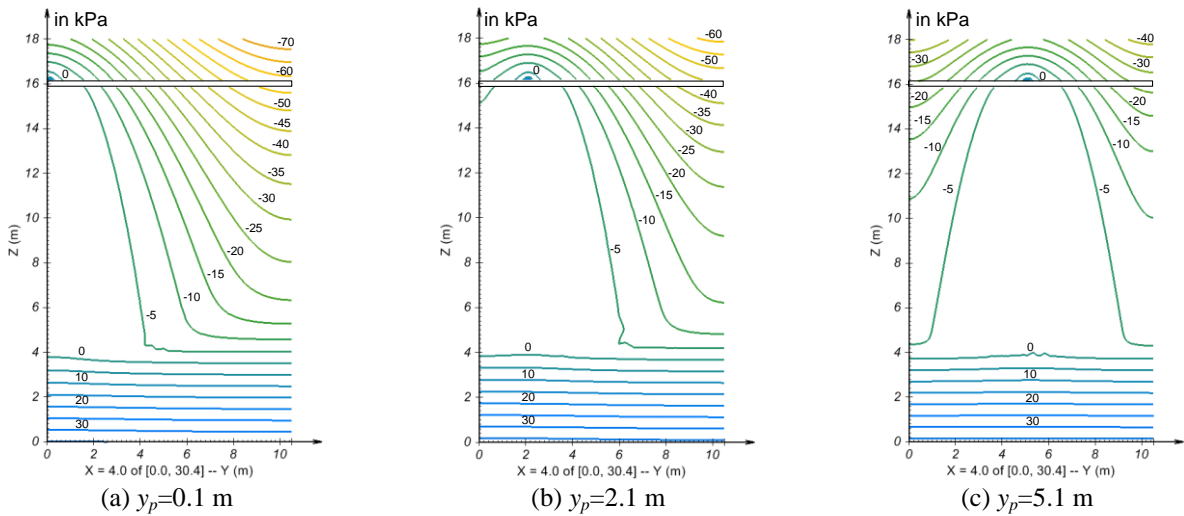
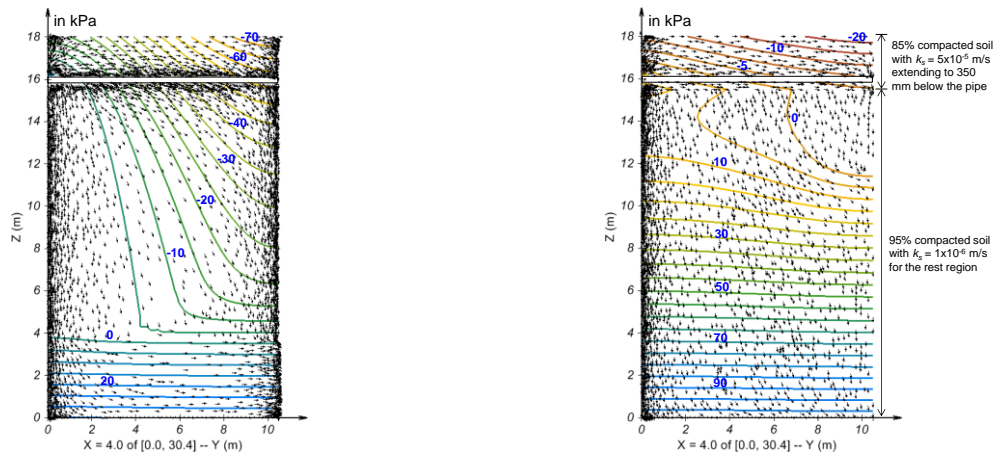


Fig. 9 Comparison of steady-state pore-water pressure contours in uniform soil at 95% relative compaction along the pipe direction subject to $p=20$ kPa for three pipe opening locations



(a) Homogeneous soil with RC = 95%

(b) Inhomogeneous soil with RC=85% for the trench backfill and RC = 95% for the rest of the ground

Fig. 10 Steady-state pore-water pressure contours and flow arrows indicating flow directions along the pipe direction subject to $p=20$ kPa

patterns of pore-water pressure contours under steady-state subject to various pipe water pressures, and locations and lengths of the opening. In accordance with the standard practice, the relative compaction of the backfill within the trench as shown in Fig. 1(b) equals 85% rather than 95%. To shed light on the effect of such density difference on the flow path, one more case with RC=85% for the soil inside the trench and down to 350 mm below the trench is carried out. Using parameters for the soils compacted at 85% and 95% in Table 1, Fig. 10 presents the pore-water pressure contours for the homogeneous and heterogeneous cases when they are under the influence of leakage at $p=20$ kPa on the crown area at $y_b=0.1$ m. The rise of groundwater table becomes more significant in the case of the backfill with RC=85%. For the RC=95% case, the soaked zone is limited around the leaking hole. The influenced zone where the suction is greatly altered (e.g. down to 5 kPa) extends to 12 m below the pipe. For the RC=85% case, the soaked zone underneath the pipe covers most part of the region. To maintain the steady state, the soaked zone extends to 7 m away laterally from the leaking hole. As the soil zone around the pipe is loosely compacted, preferential flow dominates within the loose layer, as can be clearly seen in Fig. 10(b). The leaked water is routed via this more permeable layer, implying the feasibility of installing a drainage layer for directing the leaked water in engineering practice. Due to the existence of the loose layer, suctions within the slope are destroyed more significantly compared with the homogeneous profile, leading to an unfavorable condition for the stability of the slope.

6. Computational issues associated with high hydraulic gradients

A common problem associated with pipe rupture, which generates high pore-water pressures, lies in the fact that the induced hydraulic gradient can be extremely high which can inevitably initiate serious soil erosion. As such, Darcy's law governing the laminar flow may become invalid. In the worst case, driven by large hydraulic gradients, the leaked water from the pipe can cause rupture of the cover soil.

These cases cannot be evaluated using the approach proposed in the present paper based on Darcy's law.

The scope of the present study is limited to cases without considering soil erosion around the broken hole. Prevention of internal erosion was indeed a major concern in the centrifuge test in this study. The leaking hole was surrounded by a gravel zone (Fig. 4), which was erosion resistant. Far away from the leaking point, internal erosion and fluidization are unlikely to take place in the soil at the test pipe pressure (35 kPa). No erosion hole was found in the experiment. As a result, the infiltration time and the ultimate phreatic surface are unlikely to be altered by soil erosion. If no gravel was placed around the pipe, internal erosion may take place and a concentrated leaking path may develop. Once losing some fine particles, the shear strength of the soil will decrease (Chen *et al.* 2017). Since slope stability analysis and stress-strain behaviour are not the foci of this paper, conclusions are drawn only based on seepage analysis.

To tackle the issues associated with high hydraulic gradients, some future work is needed such as the use of a discrete element method to evaluate particle losses under high hydraulic gradients during jet erosion. Previous work by Cui *et al.* (2011 and 2014) can be referred to. Laboratory testing would be highly useful to provide information on how the soil deforms subject to high hydraulic gradients, which offers physical insights on modelling pipe leakage problems over a wide range of pipe water pressures.

7. Conclusions

This study has proposed an approach to establishing a rigorous three-dimensional finite element model to simulate the water infiltration from a pressurized leaking pipe involving materials with contrasting hydraulic functions. The approach allows for adaptive refinement of element size and time step, assisted by an automatic procedure for progressive steepening of the hydraulic property function. Both transient and steady state flow analyses have been carried out. The following conclusions can be drawn:

- A transient analysis is conducted to validate the

proposed approach. Reasonable agreement between the computed results and experimental observations is achieved, which indicates that the proposed approach is valid and can be applied to other complex scenarios such as varying boundary conditions with complex geometries.

- The soil suction decreases as the leaked water infiltrates into the soil, the magnitude of reduction depending on the pipe water pressure. As the leakage develops from a hole to a long fracture, the soaked zone near the opening becomes much larger, laterally equal to the length of the opening and vertically extending to a substantial depth below the pipe. More importantly, the rise of the groundwater table in the long fracture case appears to be twice that in the small hole case.

- Regardless of the leakage location, the groundwater table in the uniform soil case with $RC = 95\%$ is only mounded slightly. The maximum suction that is remained at the ground surface under the influence of leakage varies in a descending order when the opening location changes from the pipe end to the middle of the slope.

- Preferential flow dominates within the loose soil backfill around the pipe. In this heterogeneous profile, the soaked zone underneath the pipe covers most part of the region. To maintain the steady state, the soaked zone extends to 7 m away laterally from the leaking hole. The leaked water is routed via this more permeable layer, which indicates the feasibility of installing a coarse sandy gravel layer for directing the leaked water in engineering practice. The presence of the drainage layer leads to a substantial reduction of suction within the slope, compared with the homogeneous soil profile.

- The analysis results in this paper have engineering implications via (1) delivering a picture on how the pore-water pressure regime develops in three dimensions, affected by pipe pressures of different magnitudes, and the location and size of the broken hole, (2) emphasizing the importance of good compaction of the soil around the pipe to prevent lateral spreading of leaking water (Fig. 10), (3) highlighting the possibility of high gradients around the pipe hence the need for erosion prevention measures, and (4) serving as basis for engineers to detect approximate locations of pipe leakage.

Acknowledgments

The work described in this paper was supported by the Construction Industry Council (Grant No. CIC15EG02) and the Research Grants Council of the Hong Kong Special Administrative Region (No. C6012-15G).

References

- Ali, A., Huang, J.S., Lyamin, A.V., Sloan, S.W. and Cassidy, M.J. (2014), "Boundary effects of rainfall-induced landslides", *Comput. Geotech.*, **61**, 341-354.
- Baker, D.L. (2006), "General validity of conductivity means in unsaturated flow models", *J. Hydrol. Eng.*, **11**(6), 526-538.
- Bathe, K.J. and Khoshgoftaar, M.R. (1979), "Finite element free surface seepage analysis without mesh iteration", *Int. J. Numer. Anal. Meth. Geomech.*, **3**(1), 13-22.
- Cassa, A.M. and Van Zyl, J.E. (2013), "Predicting the head-leakage slope of cracks in pipes subject to elastic deformations", *J. Water Supply Res. T. Aqua*, **62**(4), 214-223.
- Chen, C., Zhang, L.M. and Chang, D.S. (2016), "Stress-strain behaviour of granular soils subjected to internal erosion", *J. Geotech. Geoenviron. Eng.*, **142**(12), 06016014.
- Cheng, Y.G., Phoon, K.K. and Tan, T.S. (2008), "Unsaturated soil seepage analysis using a rational transformation method with under-relaxation", *Int. J. Geomech.*, **8**(3), 207-212.
- Cui Y., Nouri A., Chan D. and Rahmati E. (2016), "A new approach to DEM simulation of sand production", *J. Petrol. Sci. Eng.*, **147**, 56-67.
- Cui, X., Li, J., Chan, A. and Chapman, D. (2011), *Numerical Simulation of a Pipe Leakage Problem with Cohesive Particles, in Particulate Materials: Synthesis, Characterisation, Processing and Modelling*, 265-270.
- Cui, X., Li, J., Chan, A. and Chapman, D. (2014), "Coupled DEM-LBM simulation of internal fluidisation induced by a leaking pipe", *Powder Technol.*, **254**, 299-306.
- ETWB (2006), *Environment, Transport and Works Bureau, Code of Practice on Monitoring and Maintenance of Water-Carrying Services Affecting Slopes*, The Government of the Hong Kong SAR, Hong Kong.
- Fredlund, D.G. and Xing, A. (1994), "Equations for the soil-water characteristic curve", *Can. Geotech. J.*, **31**(4), 521-532.
- Geotechnical Engineering Office (1977), *Report on the Slope Failures at Sau Mau Ping August 1976*, Hong Kong Government Printer, Hong Kong.
- Guo, S., Zhang, T.Q., Shao, W.Y., Zhu, D.Z. and Duan, Y.Y. (2013), "Two-dimensional pipe leakage through a line crack in water distribution systems", *J. Zhejiang Univ. Sci. A*, **14**(5), 371-376.
- Lacy, S.J. and Prevost, J.H. (1987), "Flow through porous media: a procedure for locating the free surface", *Int. J. Numer. Anal. Meth. Geomech.*, **11**(6), 585-601.
- Lam, L., Fredlund, D.G. and Barbour, S.L. (1987), "Transient seepage model for saturated-unsaturated soil systems: A geotechnical engineering approach", *Can. Geotech. J.*, **24**(4), 565-580.
- Leong, E.C. and Rahardjo, H. (1997), "Permeability functions for unsaturated soils", *J. Geotech. Geoenviron. Eng.*, **123**(12), 1118-1126.
- Li, S.C., Wu, J., Xu, Z.H., Li, L.P., Huang, X., Xue, Y.G. and Wang, Z.C. (2016), "Numerical analysis of water flow characteristics after inrushing from the tunnel floor in process of karst tunnel excavation", *Geomech. Eng.*, **10**(4), 471-526.
- Paniconi, C. and Putti, M. (1994), "A comparison of Picard and Newton iteration in the numerical solution of multidimensional variably saturated flow problems", *Water Resour. Res.*, **30**(12), 3357-3374.
- PDE Solutions, Inc. (2005), *FlexPDE User Guide, Version 5.0*, Antioch, California, U.S.A.
- Phoon, K.K. (2017), "Role of reliability calculations in geotechnical design", *Georisk*, **11**(1), 4-21.
- Phoon, K.K., Tan, T.S. and Chong, P.C. (2007), "Numerical simulation of Richards equation in partially saturated porous media: Under-relaxation and mass balance", *Geotech. Geol. Eng.*, **25**(5), 525-541.
- Revil, A. and Cathles, L.M. (1999), "Permeability of shaly sands", *Water Resour. Res.*, **35**(3), 651-662.
- Richards, L.A. (1931), "Capillary conduction of liquids through porous mediums", *Physics*, **1**(5), 318-333.
- Shen, S.L. and Xu, Y.S. (2011), "Numerical evaluation of land subsidence induced by groundwater pumping in Shanghai", *Can. Geotech. J.*, **48**(9), 1378-1392.
- Shen, S.L., Wu, Y.X. and Misra, A. (2017), "Calculation of head difference at two sides of a cut-off barrier during excavation dewatering", *Comput. Geotech.*, **91**, 192-202.
- Szymkiewicz, A. (2012), *Modelling Water Flow in Unsaturated*

- Porous Media: Accounting for Nonlinear Permeability and Material Heterogeneity*, Springer Science & Business Media.
- Wood, W.L. (1993), *Introduction to Numerical Methods for Water Resources*, Oxford University Press.
- Wu, Y.X., Shen, S.L., Yin, Z.Y. and Xu, Y.S. (2015), "Characteristics of groundwater seepage with cut-off wall in gravel aquifer. II: Numerical analysis", *Can. Geotech. J.*, **52**(10), 1539-1549.
- Xiao, T., Li, D.Q., Cao, Z.J. and Tang, X.S. (2017), "Full probabilistic design of slopes in spatially variable soils using simplified reliability analysis method", *Georisk*, **11**(1), 146-159.
- Yin, J.H. (2009), "Influence of relative compaction on the permeability of completely decomposed granite in Hong Kong", *Can. Geotech. J.*, **46**(10), 1229-1235.
- Yoon, S., Lee, S.R., Kim, Y.T. and Go, G.H. (2015), "Estimation of saturated permeability of Korean weathered granite soils using a regression analysis", *Geomech. Eng.*, **9**(1), 101-113.
- Zhang, L.L., Li, J.H., Li, X., Zhang, J. and Zhu, H. (2016), *Rainfall-Induced Soil Slope Failure: Stability Analysis and Probabilistic Assessment*, CRC Press, Boca Raton, Florida, U.S.A.
- Zhu, H. and Zhang, L.M. (2015), "Evaluating suction profile in a vegetated slope considering uncertainty in transpiration", *Comput. Geotech.*, **63**, 112-120.
- Zhu, H., Zhang, L.M., Chan, K. and Chen, C. (2018), "Design safe distance between a buried pipe and a soil slope", *Proc. Inst. Civ. Eng. Geotech. Eng.*, **171**(4), 324-331.
- Zhu, H., Zhang, L.M., Zhang, L.L. and Zhou, C.B. (2013), "Two-dimensional probabilistic infiltration analysis with a spatially varying permeability function", *Comput. Geotech.*, **48**, 249-259.